· Article · Advances in Polar Science
doi: 10.13679/j.advps.2021.0045 March 2022 Vol. 33 No. 1: 71-85

Particle dynamics revealed by ^{210}Po/^{210}Pb disequilibria around Prydz Bay, the Southern Ocean in summer

CHEN Mengya, CHEN Min*, ZHENG Minfang, QIU Yusheng, ZHU Jing & QIAN Qiankun

College of Ocean and Earth Sciences, Xiamen University, Xiamen 361102, China

Received 5 September 2021; accepted 15 November 2021; published online 30 March 2022

Abstract Seawater samples were collected around Prydz Bay in summer of 2014, dissolved and particulate ^{210}Po and ^{210}Pb were measured to reveal the disequilibrium characteristics and particle dynamics. Our results show that the distribution of ^{210}Po and ^{210}Po/^{210}Pb activity ratio in the upper water is mainly affected by biological absorption or particle adsorption. An abnormal excess of ^{210}Po relative to ^{210}Pb was observed in the surface water at stations P1-2 and P2-2, which is likely to be the horizontal transport of water mass with high DPo/DPb)$_{A.R.}$ and TPo/TPb)$_{A.R.}$. In this study, the removal of particulate ^{210}Po is mainly controlled by the scavenging of dissolved ^{210}Po and the two have a linear positive correlation with the salinity, a negative linear correlation with the content of dissolved oxygen and a reciprocal relationship with the content of POC. The export flux of POC at 100 m is estimated to be 1.8–4.4 mmol·m^{-2}·d^{-1} (avg. 2.9 mmol·m^{-2}·d^{-1}) based on ^{210}Po/^{210}Pb disequilibria, with the highest value in the shelf, which is consistent with the distribution of biological productivity.

Keywords **^{210}Po/^{210}Pb disequilibria**, **^{210}Po excess**, **particle dynamics**, **POC export**, **Prydz Bay**

Citation: Chen M Y, Chen M, Zheng M F, et al. Particle dynamics revealed by ^{210}Po/^{210}Pb disequilibria around Prydz Bay , the Southern Ocean in summer. Adv Polar Sci, 2022, 33(1): 71-85, doi: 10.13679/j.advps.2021.0045

1 Introduction

^{210}Po and ^{210}Pb belong to the ^{238}U decay series, of which ^{210}Pb is the direct parent of ^{210}Po. Since the half-life of ^{210}Po (138.4 d) is much shorter than ^{210}Pb (22.3 a), the two will reach radioactive equilibrium in about 2.5 a without biogeochemical fractionation. However, ^{210}Po is more easily absorbed by plankton or adsorbed by particulate organic matter, while ^{210}Pb has a stronger affinity for inorganic components (Bacon et al., 1976; Nozaki et al., 1998). The difference in the biogeochemical behavior of ^{210}Po and ^{210}Pb leads to the variation in spatial distribution and the ^{210}Po/^{210}Pb disequilibria. ^{210}Po in the upper ocean is generally deficit with respect to ^{210}Pb. Two reasons are proposed to be responsible for this, one is that the atmospheric deposition flux of ^{210}Pb is much higher than that of ^{210}Po, and the other is that ^{210}Po is more easily absorbed by organisms or adsorbed by particles (Nozaki et al., 1998; Yang et al., 2006; Roca-Martí et al., 2018). However, excessive ^{210}Po was occasionally found in the upper waters of some sea areas (Kadko, 1993; Radakovitch et al., 1998), but the reason is not clear. Although extensive studies have been conducted on the distribution of ^{210}Po and ^{210}Pb in the ocean in recent years, due to sampling limitations, there are few reports in the Southern Ocean, especially around Prydz Bay. Yin et al. (2004) reported that the specific activities of total ^{210}Po and ^{210}Pb in the surface water around Prydz Bay ranged from 0.80 to 1.52 Bq·m^{-3} and from 1.34 to 2.15 Bq·m^{-3}, with averages of 1.14 and 1.66 Bq·m^{-3}, respectively. The ^{210}Po/^{210}Pb activity ratio in the surface water of Prydz Bay seems to be higher than the average value of other sea areas, which is attributed to the

* Corresponding author, ORCID: 0000-0003-0369-694X, E-mail: mchen@xmu.edu.cn

low atmospheric deposition flux of ^{210}Pb, the long residence time of ^{210}Po, or the horizontal transport of water masses with high ^{210}Po/^{210}Pb activity ratio (Yin et al., 2004; Yang et al., 2009; Hu, 2016).

Marine particles are carriers of biological pump. The photosynthesis of plankton in the euphotic zone drives the degradation and sedimentation of particulate organic matter in deep water. The export flux of particulate organic carbon (POC) is one of the important indicators for evaluating the efficiency of biological pump. ^{210}Po/^{210}Pb disequilibria has been widely used in estimating the export flux of POC in recent years. These estimates of the POC flux exported from the euphotic zone are between 0.04 mmol·m^{-2}·d^{-1} and 12.6 mmol·m^{-2}·d^{-1}, showing a general decrease with the increase of latitude, which may be related to the changes in biological productivity caused by light and nutrients (Charette et al., 1999; Kim and Church, 2001; Murray et al., 2005; Stewart et al., 2007; Hu et al., 2014; Roca-Martí et al., 2016; Ma et al., 2017). Although the data around Prydz Bay is limited, the POC flux exported from the euphotic zone estimated from the ^{210}Po/^{210}Pb disequilibria shows a pattern that the flux inside the bay is greater than that outside (Yang et al., 2009; Hu, 2016), which is generally consistent with the spatial variation of biological activities. Regarding the ^{210}Po and ^{210}Pb in Prydz Bay, some issues such as the reason why ^{210}Po is excess with respect to ^{210}Pb in surface water at some sites, and the regulation factors of scavenging and removal of ^{210}Po are still unclear and deserve more in-depth study.

In this study, dissolved and particulate ^{210}Po and ^{210}Pb in the upper 100 m around Prydz Bay were determined to reveal the biogeochemical processes affecting the distribution of ^{210}Po and ^{210}Pb. In addition, the scavenging and removal rates of ^{210}Po are calculated based on the ^{210}Po/^{210}Pb disequilibria. The export flux of POC was further estimated to reveal the spatial variation of biological pump. In the context of the scarcity of data on the ^{210}Po/^{210}Pb disequilibria and POC export flux, our study is of great significance for understanding the particle dynamics and biological pump in the high-latitude Southern Ocean.

2 Method

2.1 Study area

Prydz Bay is located in the eastern Antarctica and belongs to the Indian Ocean Sector of Southern Ocean. It is a semi-open embayment, shaped like a triangle. Frame Bank (near 68°S, 69°E) and Four Ladies Bank (near 70°S, 76°E) are located in the west and east of Prydz Bay, respectively. The Lambert Glacier extends from land to the bay and forms the Amery Ice Shelf in the southern boundary of Prydz Bay (Anderson, 1999). The interaction of atmosphere, ice shelf, and ocean affects the hydrological characteristics of Prydz Bay (Pu et al., 2001). The water in the upper 100 m around Prydz Bay includes two water masses, Antarctic Surface Water (AASW) and Winter Water (WW). Their temperature and salinity characteristics are as follows: AASW: $31.8 < S < 34.0$, $-2°C < T < 1.5°C$; WW: $34.0 < S < 34.4$, $-2°C < T < -0.5°C$ (Smith et al., 1984). The AASW is usually distributed at a depth less than 50 m, while the WW is located at a depth of 50–100 m below AASW (Jia, 2019). In addition, the Circumpolar Deep Water (CDW) with the characteristics of high temperature and high salinity at a depth of 100–2000 m rises from the Antarctic divergence zone, transporting nutrient-rich deep water to the surface (Su, 1987; Yabuki et al., 2006; Williams et al., 2016; Jia, 2019). Previous studies have shown that chlorophyll *a* and primary productivity in surface water in the inner bay and on the slope of Prydz Bay in summer are significantly higher than those in the open ocean (Liu et al., 2004). The concentration of POC also showed a decrease from the inner bay to the outer bay, and from the surface to the deep (Hu et al., 2001). In fact, it has been found that there is a good positive correlation between POC and chlorophyll *a* around Prydz Bay, indicating the biological source of POC (Hu et al., 2001). In addition, studies on the composition of phytoplankton communities around Prydz Bay have shown that diatoms are the main dominant species in summer (Cai et al., 2005). In summary, in addition to physical processes, biological activities such as POC production and remineralization also play an important role in biogeochemical cycle around Prydz Bay in summer.

2.2 Sampling

The seawater samples were collected from the 30th Chinese National Antarctic Research Expedition (CHINARE) onboard R/V *Xuelong* from February 26 to March 5, 2014. The sampling locations are located from 72.9°E to 76.5°E in longitude and 62.4°S to 69.3°S in latitude (Figure 1). A total of 34 samples with a depth of less than 100 m were collected at 7 stations around Prydz Bay. Among them, the station IS0 is located in the bay, and the others are outside the bay. Seawater samples with a volume of 4 to 10 dm^3 at different depths were collected by CTD-Rosette. The sample was immediately filtered through a mixed cellulose ester membrane with a diameter of 47 mm and a pore size of 0.4 μm to separate the dissolved and particulate phases. The filtrate was collected in a polyethylene bottle, and then by 10–20 cm^3 of 1:1 hydrochloric acid was added to adjust the pH to ~2. The filter membrane containing the particulate matter was placed in a sealed bag and stored frozen. Both the filtrate and the filter were brought back to the land laboratory for the determination of ^{210}Po and ^{210}Pb.

2.3 Determination of ^{210}Po and ^{210}Pb

The determination of ^{210}Po and ^{210}Pb refers to Fleer and Bacon (1984) and Yang et al. (2011). In brief, after the internal standards of ^{209}Po and stable Pb were added, the

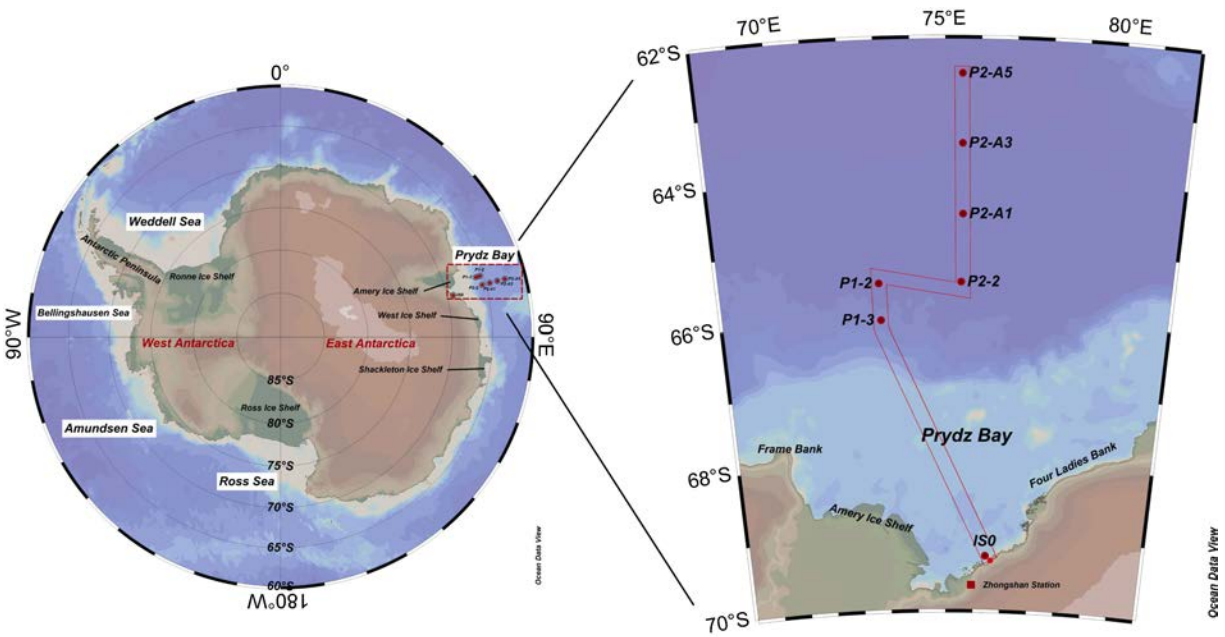

Figure 1 Sampling locations around Prydz Bay, Antarctica. The left panel shows the location of Prydz Bay. The red frame in the right panel is customized with IS0, P1-3, P1-2, P2-2, P2-A1, P2-A3, P2-A5 according to the order of station locations. The cross-sectional distribution of various parameters takes the offshore distance as horizontal axis.

^{210}Po and ^{210}Pb in the filtrate were enriched by $Fe(OH)_3$ co-precipitation. With the addition of shielding reagents and certain pH and temperature conditions, Po was self-deposited on a silver disc. The radioactivity of ^{209}Po and ^{210}Po was measured by an alpha spectrometer. The filter was digested with a mixed acid of nitric acid, perchloric acid and hydrofluoric acid at a high temperature. The subsequent treatment was the same as that of dissolved phase. The radioactivity of ^{210}Pb was calculated by measuring the ^{210}Po generated from ^{210}Pb over a period of time. That is, after the first self-deposition of Po, the sample solution was sealed and stored for more than one year to allow ^{210}Po growth. The radioactivity of the grown ^{210}Po was also measured with an alpha spectrometer. The reported activity concentrations of ^{210}Po and ^{210}Pb were corrected back to the sampling time according to Fleer and Bacon (1984). The reported error is ± 1σ counting error, and the propagation calculation has been performed. For convenience, the activity concentration of ^{210}Po in the dissolved and particle phases are denoted as DPo and PPo, respectively. Similarly, the activity concentration of ^{210}Pb in the dissolved and particle phases is represented by DPb and PPb, respectively. TPo and TPb are used to represent the total activity concentration of ^{210}Po and ^{210}Pb, respectively, where TPo = DPo + PPo and TPb = DPb + PPb.

2.4 Calculation of kinetic parameters of ^{210}Po

Here, by ignoring the effects of advection and diffusion, a simplest one-dimensional steady-state irreversible model is used to describe the mass balance of ^{210}Po (Bacon et al., 1976). The equations are as follows:

$$\frac{\partial A_{\mathrm{DPo}}}{\partial t} = A_{\mathrm{DPb}}\lambda_{\mathrm{Po}} + E_{\mathrm{Po}} - A_{\mathrm{DPo}}\lambda_{\mathrm{Po}} - J_{\mathrm{Po}}, \quad (1)$$

$$\frac{\partial A_{\mathrm{PPo}}}{\partial t} = A_{\mathrm{PPb}}\lambda_{\mathrm{Po}} + J_{\mathrm{Po}} - A_{\mathrm{PPo}}\lambda_{\mathrm{Po}} - P_{\mathrm{Po}}, \quad (2)$$

$$\frac{\partial A_{\mathrm{TPo}}}{\partial t} = A_{\mathrm{TPb}}\lambda_{\mathrm{Po}} + E_{\mathrm{Po}} - A_{\mathrm{TPo}}\lambda_{\mathrm{Po}} - P_{\mathrm{Po}}, \quad (3)$$

where A_{DPo}, A_{PPo}, A_{TPo}, A_{DPb}, A_{PPb}, and A_{TPb} represent the activity concentration of DPo, PPo, TPo, DPb, PPb, and TPb (Bq·m^{-3}), respectively. λ_{Po} is the decay constant of ^{210}Po (1.828 a^{-1}). E_{Po} represents the atmospheric deposition rate of ^{210}Po (Bq·m^{-3}·a^{-1}). J_{Po} represents the scavenging rate of dissolved ^{210}Po from dissolved to particulate phase (Bq·m^{-3}·a^{-1}). P_{Po} represents the removal rate of particulate ^{210}Po due to particle sedimentation (Bq·m^{-3}·a^{-1}). The contribution of atmospheric deposition to ^{210}Po in seawater is very small, usually accounting for only about 2% of ^{210}Po generated from ^{210}Pb decay (Masqué et al., 2002). Therefore, E_{Po} is regarded as 0 in this study, as in many previous studies (Poet et al., 1972; Nozaki et al., 1997; Verdeny et al., 2009).

When the system is in a steady state, the activity concentrations of ^{210}Po and ^{210}Pb in seawater does not change with time, at this time: $\frac{\partial A_{\mathrm{DPo}}}{\partial t} = \frac{\partial A_{\mathrm{DPo}}}{\partial t} = \frac{\partial A_{\mathrm{TPo}}}{\partial t} = 0$. Therefore, the scavenging rate, removal rate and residence time of ^{210}Po are calculated as follows:

$$J_{\mathrm{Po}} = A_{\mathrm{DPb}}\lambda_{\mathrm{Po}} - A_{\mathrm{DPo}}\lambda_{\mathrm{Po}}, \quad (4)$$

$$P_{\mathrm{Po}} = A_{\mathrm{PPb}}\lambda_{\mathrm{Po}} - A_{\mathrm{PPo}}\lambda_{\mathrm{Po}} + J_{\mathrm{Po}} = A_{\mathrm{TPb}}\lambda_{\mathrm{Po}} - A_{\mathrm{TPo}}\lambda_{\mathrm{Po}}, \quad (5)$$

$$\tau_{\mathrm{DPo}} = A_{\mathrm{DPo}} / J_{\mathrm{Po}}, \quad (6)$$

$$\tau_{PPo} = A_{PPo} / P_{Po}\,, \quad (7)$$

$$\tau_{TPo} = A_{TPo} / P_{Po}\,, \quad (8)$$

where τ_{DPo}, τ_{PPo} and τ_{TPo} represent the residence time of DPo, PPo and TPo in seawater (a), respectively.

2.5 Other parameters

The content of POC was determined in this study. Briefly, approximately 5 dm^3 of seawater samples were filtered through a pre-weighed and pre-burned (4 h at 450 °C) GF/F membrane to collect suspended particles. The sample was fumigated with hydrochloric acid for 48 h to remove inorganic carbon and washed to neutrality. After 24 h of drying, the POC was determined by an Element Analyzer (Delta V, Thermo Fisher Scientific). The standard material $C_6H_6N_2O$ was used to quantify POC content. The detection limit of POC was 0.1 μmol C, and the accuracy was better than 0.2%.

Dissolved oxygen (DO) and silicate data were downloaded from the National Arctic and Antarctic Data Center of China. The DO was measured by iodometry. When the DO concentration is greater than 550 $mmol \cdot m^{-3}$, the detection limit is 5.3 $mmol \cdot m^{-3}$, and the accuracy is ±4.0 $mmol \cdot m^{-3}$.The silicate was determined by silicomolybdic blue spectrophotometry. When the silicate concentration is 4.5 $mmol \cdot m^{-3}$, the detection limit is 0.10 $mmol \cdot m^{-3}$, and the accuracy is ± 4.0%.

3 Results

3.1 Temperature and salinity

The spatial variation of temperature and salinity at depths of above 200 m at our sites is shown in Figure 2. The temperature and salinity at the depth of 0–200 m are between −1.78°C to 1.94°C and 33.18 to 34.64, with an average of −0.27 °C and 4.10, respectively. The surface water at station IS0 located in the front of the Amery Ice Shelf has high temperature and low salinity, showing a characteristic of AASW. However, at depths greater than 100 m, the temperature decreases as the depth increases, while the salinity increases (Figure 2), which is related to the sinking and accumulation of high-density brines formed by freezing seawater in winter. A minimum temperature appears at a depth of 50–100 m at stations P1-3, P1-2, P2-2, and P2-A1, indicating the effect of cold water transporting northward. Previous studies have shown that a cold tongue with a temperature of −1.8°C is observed between AASW

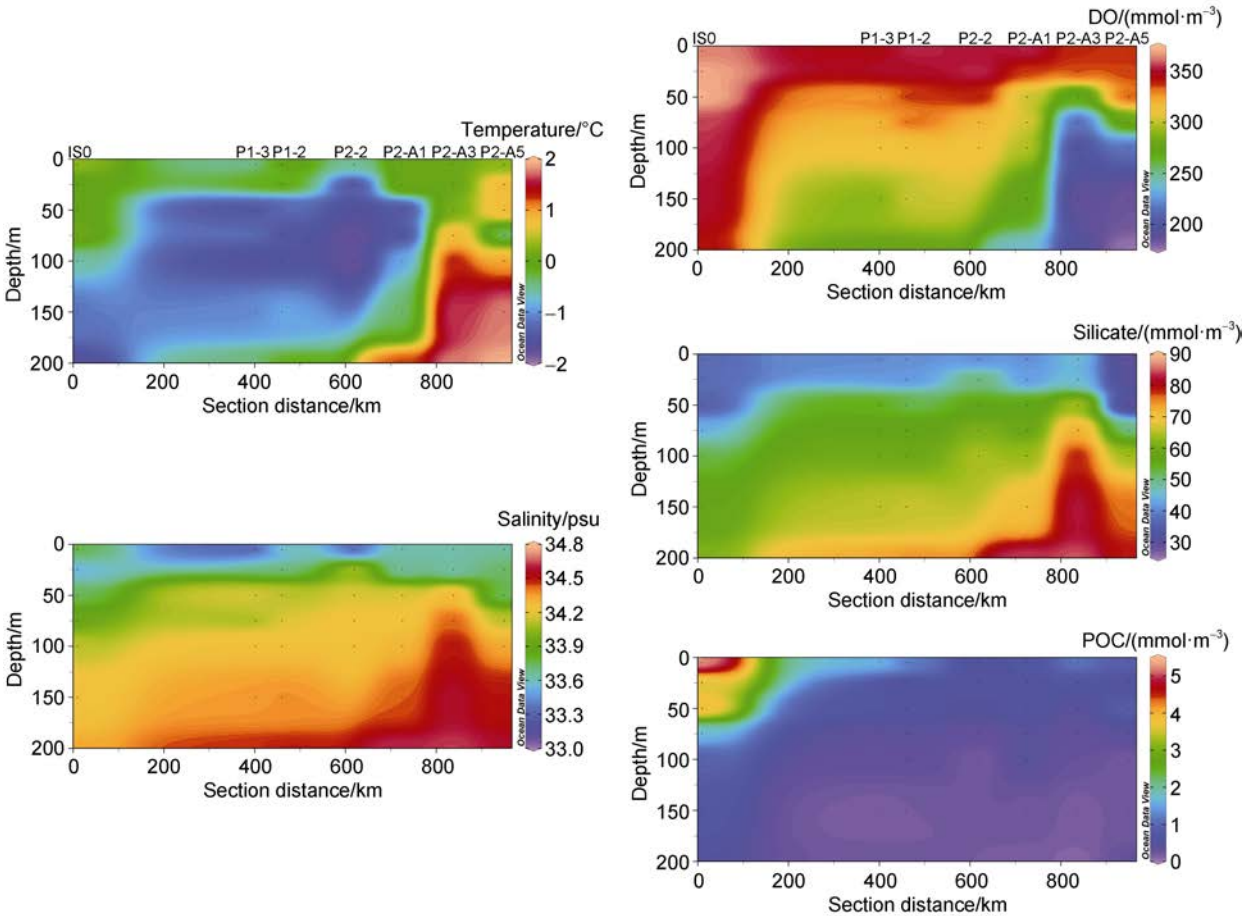

Figure 2 The sectional distribution of temperature, salinity, DO, silicate and POC in the upper 200 m water column.

and CDW at a depth of about 50 m north of 67 °S, resulting in a homogenous temperature layer with a thickness of about 50 m north of 66 °S (Pu et al., 2001). The temperature and salinity contours below 100 m at stations P2-A3 and P2-A5 protrude upward (Figure 2), indicating an upwelling of CDW.

3.2 DO, silicate and POC

The concentration of DO ranges from 176.01 mmol·m^{-3} to 372.27 mmol·m^{-3}, with an average of 305.33 mmol·m^{-3}. The DO at station IS0 is relatively high, especially at a depth of 0–50 m (Figure 2), which may reflect the influence of primary productivity. The melting of a large number of icebergs and floating ice along the coast of Prydz Bay in summer promotes the water stratification, which is conducive to the growth of phytoplankton (Sun et al., 2012). The DO concentration at stations outside the bay is higher at the surface, and decreases with increasing depth (Figure 2). The DO at stations P2-A3 and P2-A5 decreases sharply with the increasing depth at a depth of 50–200 m, similar to changes in temperature and salinity, reflecting the effect of CDW upwelling (Figure 2).

The concentration of silicate varies from 28.89 to 85.10 mmol·m^{-3}, with an average of 56.40 mmol·m^{-3}. The silicate in the bay is significantly lower than that outside the bay, which corresponds to the spatial variability of biological activities. The profiles of silicate show that the concentration generally increases with depth (Figure 2), reflecting the combined effect of absorption by phytoplankton and degradation of organic matter. The vertical changes of silicate at stations P2-A3 and P2-A5 show a significant increase at depths of 50–200 m (Figure 2), which also reflected the impact of CDW upwelling.

The POC content varies from 0.12 mmol·m^{-3} to 5.34 mmol·m^{-3}, with an average of 0.78 mmol·m^{-3}. The spatial variation of POC indicates that the POC content in the bay is significantly higher than that outside the bay (Figure 2), which is consistent with previous reports (Han et al., 2010). The profile of POC basically shows the characteristics of high surface and low depth layer, whether in the bay or outside the bay. The POC in water above 100 m varies widely, while below 100 m, the content is low and basically stable (Figure 2). The POC around Prydz Bay may mainly come from photosynthesis of plankton, which shows the differences between the inner and outer bay, and between the euphotic zone and the deep layer.

3.3 ^{210}Po

The activity concentration of TPo at a depth of 0–100 m around Prydz Bay ranges from 0.59 to 3.67 Bq·m^{-3}, with an average of 1.26 Bq·m^{-3} (Table S1). The dissolved ^{210}Po makes up a large proportion of TPo (86% ± 10%), resulting in similar spatial variability between TPo and DPo (Figure 3).

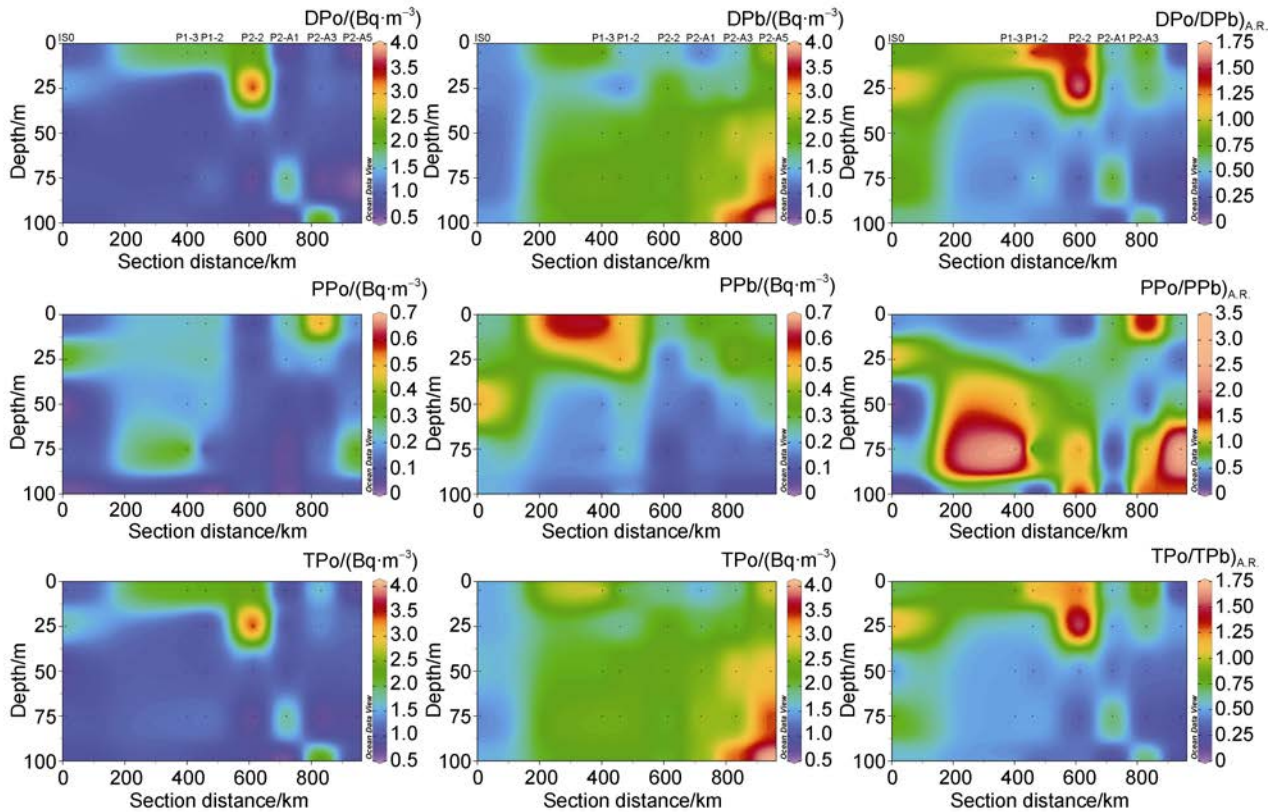

Figure 3 The sectional distribution of activity concentration and activity ratio of dissolved, particulate and total ^{210}Po and ^{210}Pb in the upper 100 m water column.

The maximum of DPo, PPo and TPo (1.43, 0.34, and 1.77 Bq·m^{-3}, respectively) at station IS0 in the bay appears at 25 m (Figure 3), corresponding to the minimum of temperature (−0.06°C), salinity (33.54) and POC content (3.52 μmol·dm^{-3}). Solar radiation, sea ice meltwater, and winter residual water together form the low temperature and low salinity in the subsurface, which weakens biological activity and particle scavenging, and retains a high ^{210}Po. In addition, the active plankton activities in surface water produce particles with high PPo, whose settling and retention forms the high PPo in the subsurface. The lowest DPo (0.75 Bq·m^{-3}), PPo (0.01 Bq·m^{-3}), and TPo (0.76 Bq·m^{-3}) at a depth of 50 m correspond to the highest POC (3.92 μmol·dm^{-3}), which may reflect the effect of enhanced biological activity on the absorption and adsorption of ^{210}Po. At stations P1-3 and P1-2, the activity concentrations of DPo and TPo in the surface layer are higher than those in the subsurface layer (Figure 3). In particular, abnormally high DPo and TPo appear in the waters above 40 m at station P2-2, which may be related to the extra input of DPo during the northward transport of the cold water mass on the shelf (Figure 3). In general, except for station P2-2, the activity concentration of DPo is the lowest in the surface layer, and increases with depth below 100 m, but the PPo at stations P2-A1, P2-A3 and P2-A5 are higher in the surface (Figure 3). The low DPo and high PPo in surface water are related to biological activity. The absorption by organisms and the adsorption by particles lead to a decrease in DPo and an increase in PPo. In the subsurface layer, the increase in DPo is accompanied by the decrease in PPo, reflecting the effect of degradation of particulate organic matter. In terms of spatial variability, the TPo and DPo in the shelf are lower than those in the slope and basin (Figure 3), indicating more active biological activities and stronger particle scavenging on the shelf.

3.4 ^{210}Pb

The activity concentrations of DPb and PPb vary from 1.11 to 4.00 Bq·m^{-3} and from 0.06 to 0.67 Bq·m^{-3}, with an average of 2.08 Bq·m^{-3} and 0.24 Bq·m^{-3}, respectively (Table S1). The distribution of DPb, PPb and TPb in the upper 100 m water column shows that DPb and TPb in surface water are lower, while PPb is higher (Figure 3), reflecting the effect of atmospheric deposition and particle scavenging, which is similar to those in the Weddell Sea and the Atlantic Ocean affected by the CDW (Somayajulu and Craig, 1976; Chung and Applequist, 1980). The atmospheric deposition of ^{210}Pb (Somayajulu and Craig, 1976; Baskaran, 2011) and the change in particle scavenging caused by the decrease in primary productivity with depth (Liu et al., 2004; Qiu et al., 2004; Sun et al., 2012) together form a mirror image between DPb (TPb) and PPb. Spatially, the activity concentrations of DPb and TPb in the bay are lower than those outside the bay, reflecting the stronger scavenging and removal of ^{210}Pb by biogenic particles in the bay. The high DPb and TPb and low PPb at depths of 50–100 m at stations P2-A3 and P2-A5 may be related to the upwelling of the CDW. Previous studies have found that the activity concentration of DPb in CDW is as high as 2–3 Bq·m^{-3} (Chung and Applequist, 1980).

4 Discussion

4.1 Characteristics of ^{210}Po/^{210}Pb activity ratio

The activity ratios of DPo/DPb $(DPo/DPb)_{A.R.}$ and PPo/PPb $(PPo/PPb)_{A.R.}$ are between 0.13 to 1.71 and between 0.01 to 3.23, and the average values are 0.59 and 0.82, respectively (Table S1). The activity ratio of TPo/TPb $(TPo/TPb)_{A.R.}$ varies from 0.21 to 1.64, with an average of 0.58. Figure 3 shows the distribution of $DPo/DPb)_{A.R.}$, $PPo/PPb)_{A.R.}$ and $TPo/TPb)_{A.R.}$ in the upper 100 m water column at our stations. Although $PPo/PPb)_{A.R.}$ varies greatly, the average $PPo/PPb)_{A.R.}$ is greater than that of $DPo/DPb)_{A.R.}$, and the activity concentration of particulate ^{210}Po is always higher than that of particulate ^{210}Pb, indicating that biological absorption or particle adsorption preferentially remove ^{210}Po compared to ^{210}Pb.

Among the stations in the bay, $DPo/DPb)_{A.R.}$, $PPo/PPb)_{A.R.}$ and $TPo/TPb)_{A.R.}$ have maximum values at a depth of 25 m, with an average of 1.15, 1.20, and 1.16, respectively, which also correspond to the maximum values of TPo. The excess of ^{210}Po at this depth indicates that organic matter degradation provides more ^{210}Po than those removed by bioabsorption and particle scavenging, thus resulting in a net input of ^{210}Po. Among the stations outside the bay, there are two cases of disequilibria between ^{210}Po and ^{210}Pb. The first case appears in the water above 20 m at station P1-2 and above 30 m at station P2-2, where DPo and TPo are excess with respect to DPb and TPb respectively, and PPo is deficient relative to PPb. The second case appears in the water above 50 m at other stations except P1-2 and P2-2, where DPo and TPo are deficient relative to DPb and TPb, respectively, indicating that ^{210}Po has a stronger affinity for particles.

The spatial variability shows that $DPo/DPb)_{A.R.}$ and $TPo/TPb)_{A.R.}$ in the waters above 50 m at each station inside and outside the bay are both less than 1, indicating that the deficits of DPo and TPo outside the bay are greater than those in the bay. Interestingly, the $PPo/PPb)_{A.R.}$ in the bay is different from that outside the bay, where it is less than 1.0 in the bay and greater than 1.0 outside the bay. The difference in the spatial distribution of $DPo/DPb)_{A.R.}$ and $PPo/PPb)_{A.R.}$ may be related to the spatial variation of biological activities. In the upper water in the bay, biological activities are intense, resulting in abundant biogenic particles, which effectively remove ^{210}Po and ^{210}Pb during sedimentation process. However, biological activities outside the bay is relatively weak, resulting the particles' removal of ^{210}Po prior to ^{210}Pb. In the 50–100 m depth interval at stations P2-A3 and P2-A5 affected by CDW upwelling, $DPo/DPb)_{A.R.}$ and $TPo/TPb)_{A.R.}$ are

significantly less than 1.0, while DPo/DPb)$_{A.R}$ is significantly greater than 1.0.

4.2 Abnormal excess of ^{210}Po in surface water

In the surface water of stations P1-2 and P2-2, DPo/DPb)$_{A.R.}$ are 1.55 and 1.43, and TPo/TPb)$_{A.R.}$ are 1.31 and 1.28, respectively, showing that ^{210}Po significantly exceeds ^{210}Pb, which is rare in previous studies. The possible reasons for the abnormal excess of ^{210}Po include four aspects, namely, the effect of upwelling, the input of sea ice meltwater, the degradation of organic matter, and the horizontal transport of water masses with high DPo/DPb)$_{A.R.}$ and TPo/TPb)$_{A.R.}$. Below we will discuss these four possibilities one by one.

The upwelling of CDW promotes the growth of phytoplankton in surface water, leading to an increase in sedimentation of organic debris. These organic debris preferentially release ^{210}Po to the deep water through the degradation of organic matter, and then enter the surface layer through the upwelling, which leads to a continuous accumulation of ^{210}Po relative to ^{210}Pb in surface water (Kadko, 1993). Although CDW upwelling was observed near 65°S outside Prydz Bay during the 9th, 15th, and 18th CHINAREs, distribution of temperature, salinity and nutrients in this voyage showed that the upwelling of CDW at stations P1-2 and P2-2 did not reach the surface (Figure 2). In addition, ^{210}Po/^{210}Pb)$_{A.R.}$ in the subsurface water at stations P1-2 and P2-2 is not higher than the surface. Therefore, the upwelling of CDW may not be a main reason for the excess of ^{210}Po in the surface water.

The input of sea ice meltwater will lead to an increase of ^{210}Po/^{210}Pb)$_{A.R.}$ in seawater, because ^{210}Pb deposited and accumulated on sea ices by atmospheric deposition undergoes radioactive decay to produce ^{210}Po. However, the reported ^{210}Po/^{210}Pb)$_{A.R.}$ in sea ice meltwater falls between 0.4 and 1.0 (Masqué et al., 2007; Roca-Martí et al., 2016; Roca-Martí et al., 2018), which cannot support the ^{210}Po excess (i.e. ^{210}Po/^{210}Pb)$_{A.R.}$ >1) observed in this study. Moreover, sea ice meltwater often promotes the growth of plankton by enhancing stratification, leading to preferential scavenging and removal of ^{210}Po, which in turn reduces ^{210}Po/^{210}Pb)$_{A.R.}$ (Roca-Martí et al., 2018). Therefore, the input of sea ice meltwater may not be the reason for the obvious excess of ^{210}Po over ^{210}Pb in the surface water we observed here.

The degradation of particulate organic matter preferentially releases ^{210}Po into seawater, resulting in an excess of ^{210}Po with respect to ^{210}Pb (Thomson and Turekian, 1976; Cochran et al., 1983; Shimmield et al., 1995; Nozaki et al., 1997; Sarin et al., 1999; Yang et al., 2009). Considering that the bioabsorption or particle scavenging in surface water is usually stronger than the degradation of organic matter, the obvious excess of ^{210}Po in surface water is also unlikely to be mainly formed by the degradation of organic matter.

After excluding the above three possibilities, the remaining possible cause is the horizontal transport of water masses with high DPo/DPb)$_{A.R.}$ and TPo/TPb)$_{A.R.}$. Note that station P2-2 is located at approximately the same latitude (65.48°S) east of station P1-2. If water masses with high ^{210}Po/^{210}Pb)$_{A.R.}$ are transported horizontally from the east or west, it can explain the obvious excess of ^{210}Po in the surface water at stations P1-2 and P2-2. However, due to the limitation of spatial resolution of our data, we are unable to determine the source of the water masses with high ^{210}Po/^{210}Pb)$_{A.R.}$, which needs further research in the future.

4.3 Particle dynamics of ^{210}Po

Based on the one-dimensional steady-state model proposed by Bacon et al. (1976), the scavenging rate, removal rate and residence time of ^{210}Po around Prydz Bay were calculated, as shown in Figure 4. Note that at 25 m at station IS0, 0 m at station P1-2, and 0 m and 25 m at station P2-2, ^{210}Po is excess with respect to ^{210}Pb, which cannot be calculated by above model. The scavenging rate, removal rate and residence time of ^{210}Po in these layers are treated as zero in Figure 4. Our calculation shows that the scavenging rate and removal rate of ^{210}Po in the waters around Prydz Bay are between 0.40 to 5.94 Bq·m^{-3}·a^{-1} and 0.31 to 5.89 Bq·m^{-3}·a^{-1}, with an average of 2.20 and 2.35 Bq·m^{-3}·a^{-1}, respectively. The residence time of DPo and PPo varies from 0.09 a to 2.36 a and from 0 to 1.71 a, respectively, with an average of 0.71 a and 0.13 a, respectively. The residence time of TPo ranges from 0.14 a to 5.47 a, with an average of 0.76 a. There is a good linear positive correlation between the scavenging rate and the removal rate: $P_{Po} = 0.89 \times J_{Po} + 0.38$ ($R^2 = 0.95$, $p < 0.0001$) (Figure 5), indicating that the removal of particulate ^{210}Po is mainly controlled by the scavenging of dissolved ^{210}Po, which is similar to that in the North Atlantic (Bacon et al., 1976). The J_{Po} and P_{Po} are lower in the entire 100 m water column at station IS0 at the front of the ice shelf, despite the higher phytoplankton biomass and primary productivity (Figure 4). The reason may be the lagging response of ^{210}Po to particle removal under the influence of sea ice and residual water in winter. In terms of spatial variability, J_{Po} and P_{Po} gradually increase from the inside to the outside of the bay, and increase with the increasing depth (Figure 4), indicating that the particles continuously scavenge and remove ^{210}Po during their settling process. The high J_{Po} and P_{Po} correspond spatially to low DPo and TPo, and high DPb, TPb and PPo/PPb)$_{A.R.}$, reflecting the upwelling of CDW not only brings dissolved ^{210}Pb, but also strengthens the scavenging of ^{210}Po. The residence times of DPo and TPo are longer in the bay, but shorter in the areas affected by the CDW upwelling (Figure 4). Except for the surface water at station P2-A3, the residence time of PPo in the entire water column is relatively short. The longer residence time of PPo in surface water of station P2-A3 corresponds to a significant excess of PPo relative to PPb, which may be the result of high PPo/PPb)$_{A.R.}$ particle input.

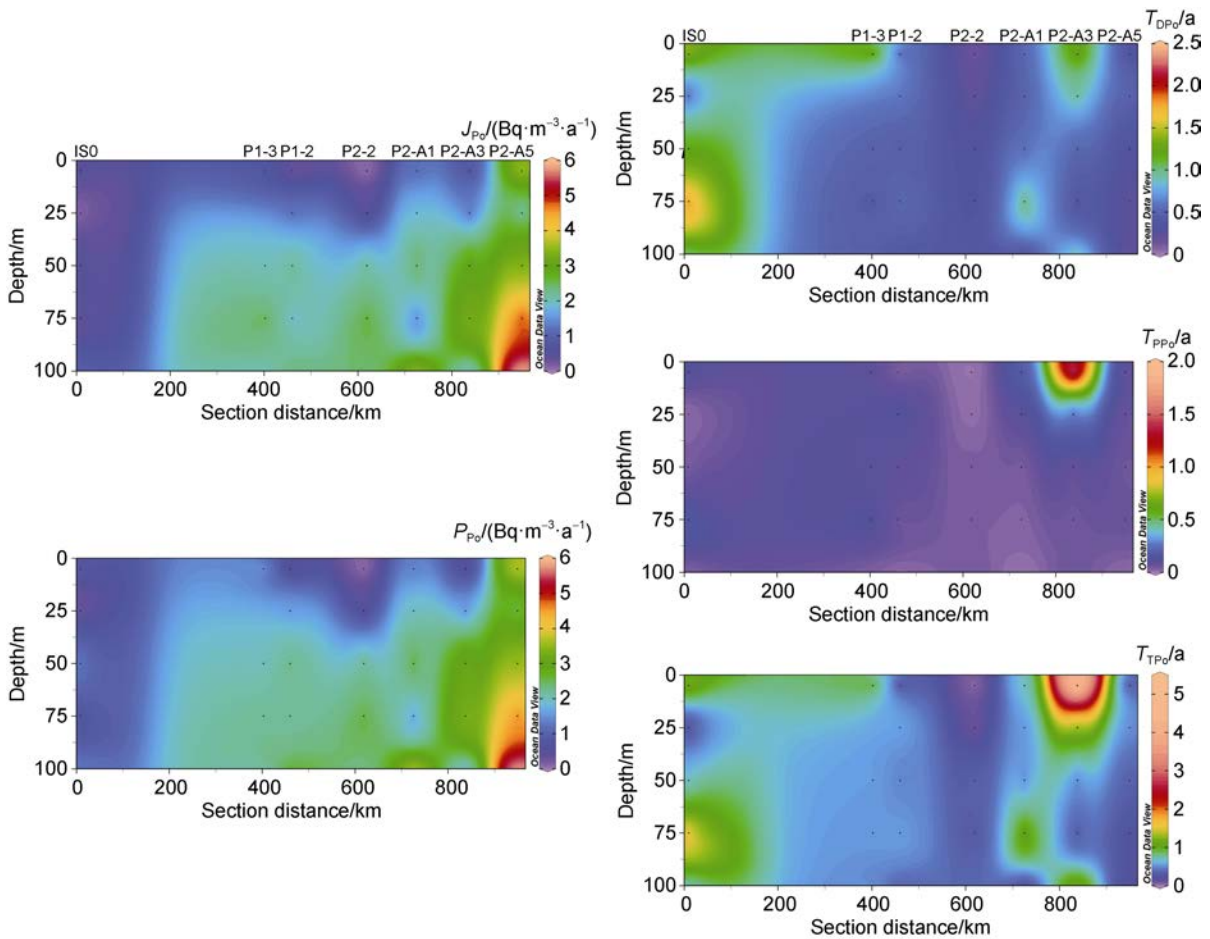

Figure 4 The sectional distribution of scavenging and removal rates of ^{210}Po, and residence times of DPo, PPo and TPo in the upper 100 m water column.

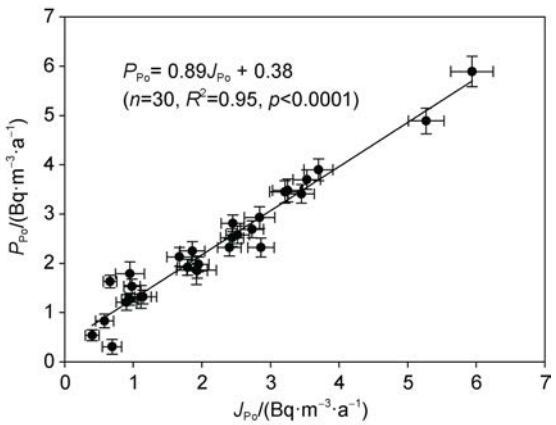

Figure 5 The relationship between scavenging rate and removal rate of ^{210}Po around Prydz Bay.

In order to reveal the factors affecting the particle dynamics of ^{210}Po around Prydz Bay, the relationship between J_{Po}, P_{Po} and temperature, salinity, dissolved oxygen (DO), silicate, and POC was explored, as shown in Figure 6 and Figure 7. In summary, J_{Po} and P_{Po} are not significantly correlated with temperature and silicate, but are significantly correlated with salinity, dissolved oxygen and POC. The positive correlation between J_{Po}, P_{Po} and salinity shows that as the salinity increases, the scavenging and removal rates of ^{210}Po increase. Since the salinity generally increases with the increasing depth, this relationship indicates that under the combined action of biological absorption and particle adsorption, the scavenging and removal rates of ^{210}Po increase with depth in the upper 100 m water column. There is a good negative linear relationship between J_{Po}, P_{Po} and dissolved oxygen. The fitting equations are as follows: $J_{Po} = -0.019 \times DO + 8.18$ ($p = 0.0003$), and $P_{Po} = -0.016 \times DO + 7.37$ ($p = 0.001$). In addition, there is a negative correlation between J_{Po}, P_{Po} and POC, and the fitting equations are as follows: $J_{Po} = 0.63/POC + 0.94$ ($p = 0.001$), and $P_{Po} = 0.52/POC + 1.32$ ($p = 0.005$). These relationships among J_{Po}, P_{Po}, DO, and POC may reflect the effect of biological processes on the geochemical fractionation between ^{210}Po and ^{210}Pb. When biological photosynthesis is stronger than the degradation of organic matter, biogenic organic matter and DO increase, which may lead to a decrease in the fractionation between ^{210}Po and ^{210}Pb and a decrease in J_{Po} and P_{Po}. On the contrary, when the degradation of organic matter is stronger than biological photosynthesis, biogenic organic matter and DO decrease, which may lead to an increase in the

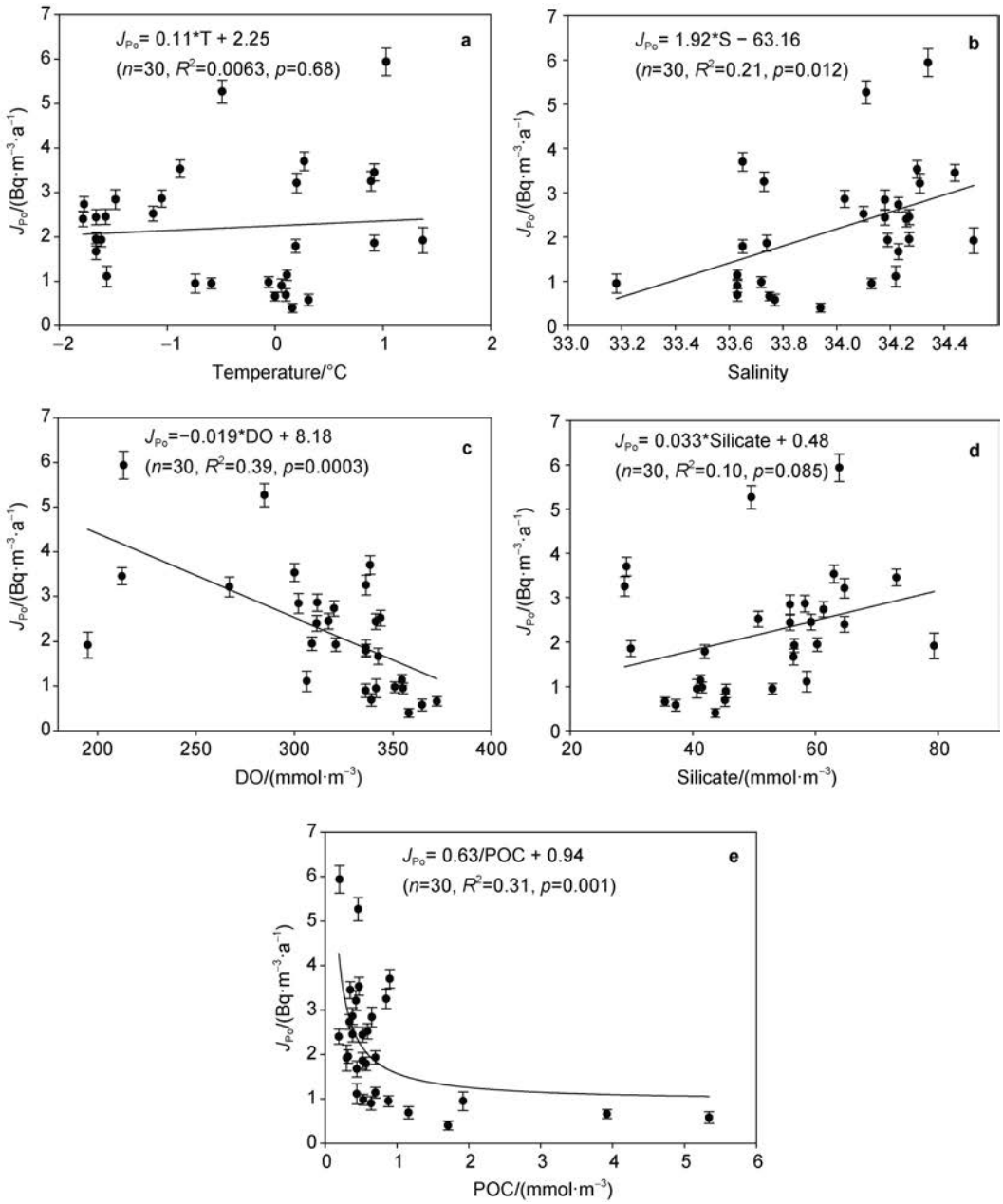

Figure 6 The relationship between scavenging rate of ^{210}Po and (**a**) temperature, (**b**) salinity, (**c**) DO, (**d**) silicate, and (**e**) POC around Prydz Bay.

fractionation between ^{210}Po and ^{210}Pb and an increase in J_{Po} and P_{Po} (Chen et al., 2021).

4.4 Estimation of POC export flux

The ^{210}Po/^{210}Pb disequilibrium has been widely used to estimate the export flux of POC in the ocean (Kim and Church, 2001; Murray et al., 2005; Hu et al., 2014; Roca-Martí et al., 2016). Here, an empirical method given by Shimmield et al. (1995) is used to calculate the POC export flux around Prydz Bay based on the removal flux of ^{210}Po. The calculation formula is as follows:

$$F_{\mathrm{POC}} = \frac{I_{\mathrm{POC}}}{I_{\mathrm{PPo}}} \cdot F_{\mathrm{Po,removal}}, \tag{9}$$

$$F_{\mathrm{Po,removal}} = \lambda_{\mathrm{Po}} \left(I_{\mathrm{TPb}} - I_{\mathrm{TPo}} \right), \tag{10}$$

where F_{POC} represents POC export flux (mmol·m^{-2}·d^{-1}). I_{POC} and I_{PPo} represent the inventory of POC (mmol·m^{-2}) and PPo (Bq·m^{-2}) in the water column, respectively. $F_{\mathrm{Po,removal}}$ represents the removal flux of particulate ^{210}Po from particle settling (Bq·m^{-2}·d^{-1}). I_{TPo} and I_{TPb} represent the inventory of TPo and TPb (Bq·m^{-2}) in the water column, respectively. As for the selection of depth interface,

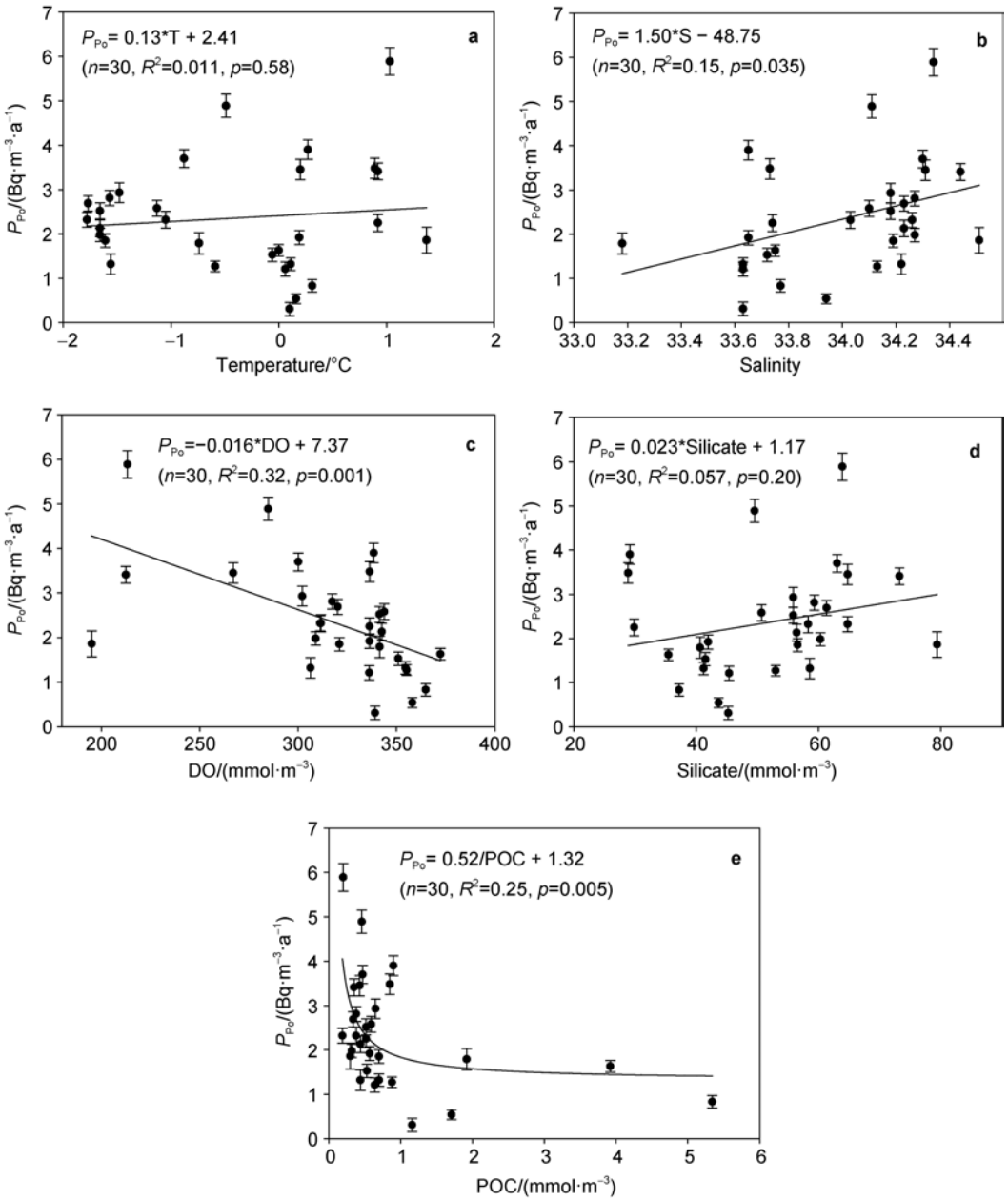

Figure 7 The relationship between removal rate of ^{210}Po and (**a**) temperature, (**b**) salinity, (**c**) DO, (**d**) silicate, and (**e**) POC around Prydz Bay.

considering that previous studies in the Bellingshausen Sea (Shimmield et al., 1995) and the Antarctic Circumpolar Current (Friedrich and van der Loeff, 2002) used 100 m as the interface, for the convenience of comparison, the POC export flux at 100 m is reported here. In addition, it has been pointed out in the above discussion that the ^{210}Po in the surface water at stations P1-2 and P2-2 may be affected by horizontal transport, which does not meet the conditions of the adopted model, so these two stations are not included in the calculation.

Our calculations show that the export flux of POC at 100 m around Prydz Bay varies from 1.8 mmol·m^{-2}·d^{-1} to 4.4 mmol·m^{-2}·d^{-1}, with an average of 2.9 mmol·m^{-2}·d^{-1}. As shown in Figure 8, the highest POC export occurs at station IS0 at the front of the ice shelf, which is consistent with the highest phytoplankton biomass and primary productivity. The lowest POC export appears at station P2-A3 outside the bay. Note that the POC export flux in the continental slope (station P1-3) is lower than that in the open ocean area (stations P2-A1 and P2-A3), which indicates that primary productivity in the open ocean may be higher than that in the continental slope during the survey period. Previous studies have shown that although the phytoplankton biomass in the continental slope outside Prydz Bay is higher

than that in the open ocean, the open ocean has a higher primary productivity due to a thicker euphotic zone (Liu et al., 2001). Therefore, the spatial variability of POC export flux may be closely related to primary production around Prydz Bay.

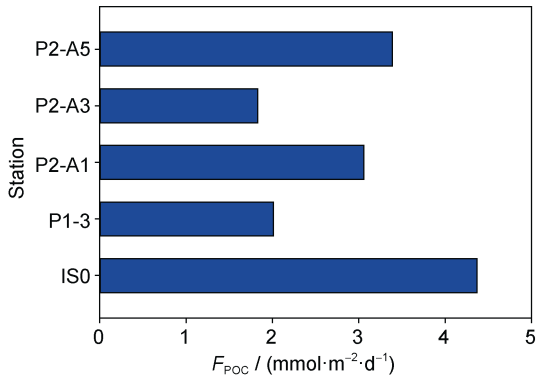

Figure 8 The POC export flux at each station around Prydz Bay estimated from ^{210}Po/^{210}Pb disequilibria.

The export flux of POC around Prydz Bay has been estimated through ^{210}Po/^{210}Pb disequilibria prior to this study. The comparison shows that the estimated POC export flux here is consistent with the report in the open ocean outside Prydz Bay (2.3 mmol·m^{-2}·d^{-1}, one site at 64.0 °S, 73.0 °E, Yang et al., 2009), but slightly lower than the reports containing more shelf stations (4.2–9.0 mmol·m^{-2}·d^{-1}, avg. 6.9 mmol·m^{-2}·d^{-1}, 68.0°S–64.0°S, 76.0°E–79.0°E) (Hu et al., 2021). Table S2 shows that the estimated POC export fluxes are lower in the high-latitude regions and increase with the decreasing latitude due to the changes in biological productivity induced by light or nutrients. It is worth noting that the export flux of POC based on ^{210}Po/^{210}Pb disequilibria is significantly lower than that based on ^{234}Th/^{238}U disequilibria (52.6–185.6 mmol·m^{-2}·d^{-1}, avg. 104.7 mmol·m^{-2}·d^{-1}) (He et al., 2008), which may reflect the difference in time scale and geochemical behavior between ^{210}Po and ^{234}Th. Ceballos-Romero et al. (2016) compared the POC export fluxes obtained by the ^{234}Th/^{238}U method, ^{210}Po/^{210}Pb method and the sediment trap in the North Atlantic, and found that the results obtained by different methods differ by orders of magnitude except for the consistency in the late bloom, which is attributed to the different time scales of nuclides and the different growth stages of phytoplankton. Regarding the three methods for estimating POC export flux, sediment trap is a most direct tool to obtain POC export, which is susceptible to several factors such as hydrodynamics, biological predation, and particle dissolution (Buesseler et al., 2007). The ^{234}Th/^{238}U disequilibria is more suitable for flux estimation under short time scale (seasonal) and high POC export. Studies have shown that in the case of low POC export flux, the results obtained by ^{234}Th/^{238}U disequilibria are often higher than those by sediment trap (Stewart et al., 2010). ^{210}Po ($T_{1/2}$ = 138.4 d) has a longer half-life than ^{234}Th ($T_{1/2}$ = 24.1 d) and is used to track the POC export on a seasonal or interannual time scale. In addition, ^{210}Po is more biologically active than ^{234}Th, which means that ^{210}Po may be more suitable for tracking POC export (Le Moigne et al., 2013).

5 Conclusions

The spatial variation of ^{210}Po and ^{210}Pb and their disequilibria in the upper 100 m water column around Prydz Bay in the summer of 2014 were studied. We found the abnormal phenomenon in the surface water at some stations that ^{210}Po is excess with respect to ^{210}Pb, which probably reflects the impact of horizontal transport of water masses with high $(DPo/DPb)_{A.R.}$ and high $(TPo/TPb)_{A.R.}$ The scavenging and removal rates of ^{210}Po vary from 0.40 to 5.94 Bq·m^{-3}·a^{-1} (average 2.2 Bq·m^{-3}·a^{-1}) and from 0.31 to 5.89 Bq·m^{-3}·a^{-1} (average 2.35 Bq·m^{-3}·a^{-1}), respectively. There is a good linear positive correlation between the two rates, indicating that the removal of particulate ^{210}Po is mainly controlled by the scavenging process from the dissolved to particulate phase. The scavenging and removal rates of ^{210}Po is positively correlated with salinity and negatively correlated with dissolved oxygen and POC, indicating that biological activities have caused biogeochemical fractionation between ^{210}Po and ^{210}Pb. Based on the ^{210}Po/^{210}Pb disequilibria, the POC export flux at 100 m around Prydz Bay is estimated to vary from 1.8 to 4.4 mmol·m^{-2}·d^{-1}, showing a feature of being higher in the bay than outside the bay.

Acknowledgements We would like to thank the captains and crews of the R/V *Xuelong* for their assistance in sampling. Data on temperature, salinity, dissolved oxygen and silicate are provided by National Arctic and Antarctic Data Center of China. This work was financially supported by National Polar Special Program "Impact and Response of Antarctic Seas to Climate Change" (Grant nos. IRASCC 01-01-02C, 02-01-01), was supported by National Natural Science Foundation of China (Grant no. 41721005), and the program funded by China Ocean Mineral Resources R & D Association (Grant no. DY135-13-E2-03). The authors also thank two anonymous reviewers, and Guest Editor Dr. Jianfeng He for their constructive comments.

References

Anderson J B. 1999. Antarctic marine geology. Cambridge: Cambridge University Press, doi: 10.1016/S0025-3227(00)00098-0.

Bacon M P, Spencer D W, Brewer P G. 1976. ^{210}Pb/^{226}Ra and ^{210}Po/^{210}Pb disequilibria in seawater and suspended particulate matter. Earth Planet Sci Lett, 32(2): 277-296, doi:10.1016/0012-821X(76)90068-6.

Baskaran M. 2011. Po-210 and Pb-210 as atmospheric tracers and global atmospheric Pb-210 fallout: a review. J Environ Radioact, 102(5): 500-513, doi:10.1016/j.jenvrad.2010.10.007.

Buesseler K O, Antia A N, Chen M, et al. 2007. An assessment of the use of sediment traps for estimating upper ocean particle fluxes. J Mar Res,

65(3): 345-416, doi:10.1357/002224007781567621.

Cai Y M, Ning X R, Zhu G H, et al. 2005. Size fractionated biomass and productivity of phytoplankton and new production in the Prydz Bay and the adjacent Indian sector of the Southern Ocean during the austral summer of 1998/1999. Acta Oceanol Sin, 27(4): 135-147 (in Chinese with English abstract).

Ceballos-Romero E, Le Moigne F A C, Henson S, et al. 2016. Influence of bloom dynamics on particle export efficiency in the North Atlantic: a comparative study of radioanalytical techniques and sediment traps. Mar Chem, 186: 198-210, doi:10.1016/j.marchem.2016.10.001.

Charette M A, Moran S B, Bishop J K B. 1999. ^{234}Th as a tracer of particulate organic carbon export in the subarctic northeast Pacific Ocean. Deep Sea Res Part II Top Stud Oceanogr, 46(11-12): 2833-2861, doi:10.1016/S0967-0645(99)00085-5.

Chen M Y, Chen M, Zheng M F, et al. 2021. ^{210}Po/^{210}Pb disequilibria influenced by production and remineralization of particulate organic matter around Prydz Bay, Antarctica. Deep Sea Res Part II Top Stud Oceanogr, 191-192: 104961, doi:10.1016/j.dsr2.2021.104961.

Chung Y, Applequist M D. 1980. ^{226}Ra and ^{210}Pb in the Weddell Sea. Earth Planet Sci Lett, 49(2): 401-410, doi:10.1016/0012-821X(80)90082-5.

Cochran J K, Bacon M P, Krishnaswami S, et al. 1983. ^{210}Po and ^{210}Pb distributions in the central and eastern Indian Ocean. Earth Planet Sci Lett, 65(2): 433-452, doi:10.1016/0012-821X(83)90180-2.

Fleer A P, Bacon M P. 1984. Determination of ^{210}Pb and ^{210}Po in seawater and marine particulate matter. Nucl Instrum Methods Phys Res, 223(2-3): 243-249, doi:10.1016/0167-5087(84)90655-0.

Friedrich J, van der Loeff M M R. 2002. A two-tracer (^{210}Po-^{234}Th) approach to distinguish organic carbon and biogenic silica export flux in the Antarctic Circumpolar Current. Deep Sea Res Part I Oceanogr Res Pap, 49(1): 101-120, doi:10.1016/S0967-0637(01)00045-0.

Han Z B, Hu C Y, Yu W, et al. 2010. Decmposition of organic carbon and inorganic carbon beneath euphotic zone in Prydz Bay, Antarctica. Chin J Polar Res, 22(3): 254-261 (in Chinese with English abstract).

He J H, Ma H, Chen L Q, et al. 2008. The investigation on particulate organic carbon fluxes with disequilibria between thorium-234 and uranium-238 in the Prydz Bay, the Southern Ocean. Acta Oceanol Sin, 27(2): 21-29 (in Chinese with English abstract).

Hu C Y, Zhang H S, Pan J M. 2001. The biogeochemistry of carbon cycle in summer of the Prydz Bay, Antarctica Ⅱ: characteristics of POC distribution. Chin J Polar Res, 13(3): 195-204 (in Chinese with English abstract).

Hu H N. 2016. Distribution of ^{210}Po and ^{210}Pb in the Prydz Bay and its adjacent sea areas and their estimate of particulate organic matter export. M.S. thesis, Xiamen, China: Xiamen University (in Chinese).

Hu H N, Liu X, Ren C Y, et al. 2021. ^{210}Po/^{210}Pb disequilibria and its estimate of particulate organic carbon export around Prydz Bay, Antarctica. Front Mar Sci, 8: 701014, doi:10.3389/fmars.2021.701014.

Hu W J, Chen M, Yang W F, et al. 2014. Enhanced particle scavenging in deep water of the Aleutian Basin revealed by ^{210}Po-^{210}Pb disequilibria. J Geophys Res Oceans, 119(6): 3235-3248, doi:10.1002/2014JC009819.

Jia R M. 2019. Spatial and temporal variations of freshwater components around the Prydz Bay, Antarctica and its implication for marine processes. Ph. D. thesis, Xiamen, China: Xiamen University (in Chinese).

Kadko D. 1993. Excess ^{210}Po and nutrient recycling within the California coastal transition zone. J Geophys Res, 98(C1): 857-864, doi:10.1029/92JC01932.

Kim G, Church T M. 2001. Seasonal biogeochemical fluxes of ^{234}Th and ^{210}Po in the upper Sargasso Sea: influence from atmospheric iron deposition. Global Biogeochem Cycles, 15(3): 651-661, doi:10.1029/2000GB001313.

Le Moigne F A C, Villa-Alfageme M, Sanders R J, et al. 2013. Export of organic carbon and biominerals derived from ^{234}Th and ^{210}Po at the Porcupine Abyssal Plain. Deep Sea Res Part I Oceanogr Res Pap, 72: 88-101, doi: 10.1016/j.dsr.2012.10.010.

Liu C G, Ning X R, Sun J, et al. 2004. Size structure of standing stock and productivity and new production of phytoplankton in the Prydz Bay and the adjacent Indian sector of the Southern Ocean during the austral summer of 2001/2002. Acta Oceanol Sin, 26(6): 107-117 (in Chinese with English abstract).

Liu Z L, Cai Y M, Ning X R, et al. 2001. Primary productivity and standing stock of phytoplankton in the Prydz Bay and the adjacent northern sea area during the austral summer of 1999/2000. Chin J Polar Res, 13(1): 1-12 (in Chinese with English abstract).

Ma H Y, Yang W F, Zhang L H, et al. 2017. Utilizing ^{210}Po deficit to constrain particle dynamics in mesopelagic water, western South China Sea. Geochem Geophys Geosyst, 18(4): 1594-1607, doi:10.1002/2017GC006899.

Masqué P, Cochran J K, Hirschberg D J, et al. 2007. Radionuclides in Arctic sea ice: tracers of sources, fates and ice transit time scales. Deep Sea Res Part I Oceanogr Res Pap, 54(8): 1289-1310, doi:10.1016/j.dsr.2007.04.016.

Masqué P, Sanchez-Cabeza J A, Bruach J M, et al. 2002. Balance and residence times of ^{210}Pb and ^{210}Po in surface waters of the northwestern Mediterranean Sea. Cont Shelf Res, 22(15): 2127-2146, doi:10.1016/S0278-4343(02)00074-2.

Murray J W, Paul B, Dunne J P, et al. 2005. ^{234}Th, ^{210}Pb, ^{210}Po and stable Pb in the central equatorial Pacific: tracers for particle cycling. Deep Sea Res Part I Oceanogr Res Pap, 52(11): 2109-2139, doi:10.1016/j.dsr.2005.06.016.

Nozaki Y, Dobashi F, Kato Y, et al. 1998. Distribution of Ra isotopes and the ^{210}Pb and ^{210}Po balance in surface seawaters of the mid Northern Hemisphere. Deep Sea Res Part I Oceanogr Res Pap, 45(8): 1263-1284, doi:10.1016/S0967-0637(98)00016-8.

Nozaki Y, Zhang J, Takeda A. 1997. ^{210}Pb and ^{210}Po in the equatorial Pacific and the Bering Sea: the effects of biological productivity and boundary scavenging. Deep Sea Res Part II Top Stud Oceanogr, 44(9-10): 2203-2220, doi:10.1016/S0967-0645(97)00024-6.

Poet S E, Moore H E, Martell E A. 1972. Lead 210, bismuth 210, and polonium 210 in the atmosphere: accurate ratio measurement and application to aerosol residence time determination. J Geophys Res, 77(33): 6515-6527, doi:10.1029/JC077i033p06515.

Pu S Z, Dong Z Q, Hu X M, et al. 2001. Upper layer waters and their northward extension from Prydz Bay in summer. Chin J Polar Sci, 12(2): 89-98 (in Chinese with English abstract).

Qiu Y S, Huang Y P, Liu G S, et al. 2004. Spatial and temporal variations of primary productivity in Prydz Bay and its adjacent sea area, Antarctica. J Xiamen Univ Nat Sci, 43(5): 676-681 (in Chinese with English abstract).

Radakovitch O, Cherry R D, Heyraud M, et al. 1998. Unusual ^{210}Po/^{210}Pb ratios in the surface water of the Gulf of Lions. Oceanol Acta, 21(3): 459-468, doi:10.1016/S0399-1784(98)80030-3.

Roca-Martí M, Puigcorbé V, Friedrich J, et al. 2018. Distribution of ^{210}Pb and ^{210}Po in the Arctic water column during the 2007 sea-ice minimum: particle export in the ice-covered basins. Deep Sea Res Part I Oceanogr Res Pap, 142: 94-106, doi:10.1016/j.dsr.2018.09.011.

Roca-Martí M, Puigcorbé V, van der Loeff M M R, et al. 2016. Carbon export fluxes and export efficiency in the central Arctic during the record sea-ice minimum in 2012: a joint ^{234}Th/^{238}U and ^{210}Po/^{210}Pb study. J Geophys Res Oceans, 121(7): 5030-5049, doi:10.1002/2016jc011816.

Sarin M M, Kim G, Church T M. 1999. ^{210}Po and ^{210}Pb in the south-equatorial Atlantic: distribution and disequilibrium in the upper 500 m. Deep Sea Res Part II Top Stud Oceanogr, 46(5): 907-917, doi:10.1016/S0967-0645(99)00008-9.

Shimmield G B, Ritchie G D, Fileman T W. 1995. The impact of marginal ice zone processes on the distribution of ^{210}Pb, ^{210}Po and ^{234}Th and implications for new production in the Bellingshausen Sea, Antarctica. Deep Sea Res Part II Top Stud Oceanogr, 42(4-5): 1313-1335, doi:10.1016/0967-0645(95)00071-W.

Smith N R, Dong Z Q, Kerry K R, et al. 1984. Water masses and circulation in the region of Prydz Bay, Antarctica. Deep Sea Res A Oceanogr Res Pap, 31(9): 1121-1147, doi:10.1016/0198-0149(84) 90016-5.

Somayajulu B L K, Craig H. 1976. Particulate and soluble ^{210}Pb activities in the deep sea. Earth Planet Sci Lett, 32(2): 268-276, doi:10.1016/0012-821X(76)90067-4.

Stewart G, Cochran J K, Xue J H, et al. 2007. Exploring the connection between ^{210}Po and organic matter in the northwestern Mediterranean. Deep Sea Res Part I Oceanogr Res Pap, 54(3): 415-427, doi:10.1016/j.dsr.2006.12.006.

Stewart G M, Moran S B, Lomas M W. 2010. Seasonal POC fluxes at BATS estimated from ^{210}Po deficits. Deep Sea Res Part I Oceanogr Res Pap, 57(1): 113-124, doi:10.1016/j.dsr.2009.09.007.

Su Y F. 1987. Upwelling of the deep water in the Prydz Bay and offshore in the Antarctic during the austral summer. Trans Oceanol Limnol, (2): 17-24, doi:10.13984/j.cnki.cn37-1141.1987.02.003 (in Chinese with English abstract).

Sun W P, Hu C Y, Han Z B, et al. 2012. Distribution of nutrients and chl *a* in Prydz Bay during the austral summer of 2011. Chin J Polar Res, 24(2): 178-186 (in Chinese with English abstract).

Thomson J, Turekian K K. 1976. ^{210}Po and ^{210}Pb distributions in ocean water profiles from the Eastern South Pacific. Earth Planet Sci Lett, 32(2): 297-303, doi:10.1016/0012-821X(76)90069-8.

van der Loeff M M R, Friedrich J, Bathmann U V. 1997. Carbon export during the Spring Bloom at the Antarctic Polar Front, determined with the natural tracer 234Th. Deep Sea Res Part II Top Stud Oceanogr, 44(1-2): 457-478, doi:10.1016/S0967-0645(96)00067-7.

Verdeny E, Masqué P, Garcia-Orellana J, et al. 2009. POC export from ocean surface waters by means of ^{234}Th/^{238}U and ^{210}Po/^{210}Pb disequilibria: a review of the use of two radiotracer pairs. Deep Sea Res Part II Top Stud Oceanogr, 56(18): 1502-1518, doi:10.1016/j.dsr2.2008.12.018.

Williams G, Herraiz-Borreguero L, Roquet F, et al. 2016. The suppression of Antarctic bottom water formation by melting ice shelves in Prydz Bay. Nat Commun, 7: 1-9, doi: 10.1038/ncomms12577.

Yabuki T, Suga T, Hanawa K, et al. 2006. Possible source of the Antarctic bottom water in the Prydz Bay Region. J Oceanogr, 62(5): 649-655, doi:10.1007/s10872-006-0083-1.

Yang W F, Huang Y P, Chen M, et al. 2006. Disequilibria between ^{210}Po and ^{210}Pb in surface waters of the southern South China Sea and their implications. Sci China Ser D, 49(1): 103-112, doi:10.1007/s11430-004-5233-y.

Yang W F, Huang Y P, Chen M, et al. 2009. Export and remineralization of POM in the Southern Ocean and the South China Sea estimated from ^{210}Po/^{210}Pb disequilibria. Chin Sci Bull, 54(12): 2118-2123, doi:10.1007/s11434-009-0043-4.

Yang W F, Huang Y P, Chen M, et al. 2011. Carbon and nitrogen cycling in the Zhubi coral reef lagoon of the South China Sea as revealed by ^{210}Po and ^{210}Pb. Mar Pollut Bull, 62(5): 905-911, doi:10.1016/j.marpolbul.2011.02.058.

Yin M D, Zeng W Y, Wu S Y, et al. 2004. Distribution of uranium-series isotopes in the Prydz Bay, Antarctica. Chin J Polar Res, 16(1): 11-21 (in Chinese with English abstract).

Supporting information: supplementary tables

Table S1 The activity concentrations and activity ratio of dissolved, particulate and total ^{210}Po and ^{210}Pb around Prydz Bay

Stations	Layer	DPo/(Bq·m^{-3})	PPo/(Bq·m^{-3})	TPo/(Bq·m^{-3})	DPb/(Bq·m^{-3})	PPb/(Bq·m^{-3})	TPb/(Bq·m^{-3})	DPo/DPb)$_{A.R.}$	PPo/PPb)$_{A.R.}$	TPo/TPb)$_{A.R.}$
IS0	0	0.97±0.09	0.11±0.03	1.08±0.09	1.28±0.10	0.25±0.03	1.53±0.10	0.75±0.09	0.45±0.15	0.70±0.08
	25	1.43±0.09	0.34±0.05	1.77±0.10	1.24±0.09	0.28±0.04	1.53±0.10	1.15±0.11	1.20±0.24	1.16±0.10
	50	0.75±0.05	0.01±0.04	0.76±0.07	1.11±0.08	0.54±0.07	1.65±0.11	0.68±0.07	0.02±0.08	0.46±0.05
	75	0.94±0.06	0.12±0.03	1.06±0.07	1.16±0.08	0.20±0.03	1.36±0.09	0.81±0.08	0.60±0.16	0.78±0.07
	100	0.84±0.06	0.03±0.02	0.86±0.06	1.35±0.10	0.21±0.03	1.56±0.10	0.62±0.06	0.13±0.11	0.55±0.06
P1-3	0	1.95±0.09	0.21±0.06	2.17±0.11	2.47±0.19	0.67±0.09	3.14±0.21	0.79±0.07	0.32±0.09	0.69±0.06
	50	0.88±0.05	0.17±0.02	1.06±0.05	1.94±0.14	0.13±0.02	2.07±0.14	0.46±0.04	1.32±0.26	0.51±0.04
	75	0.79±0.05	0.43±0.05	1.21±0.07	2.35±0.18	0.13±0.02	2.48±0.18	0.33±0.03	3.23±0.59	0.49±0.04
	100	1.05±0.05	0.08±0.02	1.13±0.06	2.11±0.14	0.10±0.02	2.21±0.14	0.49±0.04	0.83±0.25	0.51±0.04
P1-2	0	1.94±0.07	0.25±0.06	2.19±0.09	1.25±0.10	0.43±0.06	1.68±0.11	1.55±0.13	0.59±0.15	1.31±0.10
	25	0.70±0.07	0.25±0.06	0.94±0.09	1.23±0.09	0.55±0.07	1.78±0.12	0.56±0.07	0.45±0.12	0.53±0.06
	50	0.79±0.05	0.23±0.04	1.01±0.06	2.17±0.16	0.26±0.04	2.42±0.17	0.36±0.04	0.88±0.19	0.42±0.04
	75	1.28±0.06	0.01±0.02	1.29±0.07	2.19±0.17	0.26±0.03	2.46±0.17	0.58±0.05	0.05±0.09	0.52±0.05
	100	0.78±0.05	0.01±0.02	0.79±0.05	2.12±0.16	0.21±0.03	2.33±0.17	0.37±0.04	0.05±0.09	0.34±0.03
P2-2	0	2.30±0.11	0.07±0.02	2.37±0.11	1.61±0.13	0.25±0.03	1.86±0.13	1.43±0.13	0.27±0.09	1.28±0.11
	25	3.58±0.17	0.09±0.02	3.67±0.18	2.09±0.15	0.15±0.02	2.24±0.15	1.71±0.15	0.62±0.17	1.64±0.14
	50	0.88±0.06	0.12±0.02	1.00±0.07	2.22±0.16	0.16±0.02	2.38±0.16	0.40±0.04	0.74±0.17	0.42±0.04
	75	0.57±0.04	0.09±0.02	0.65±0.05	2.06±0.16	0.06±0.01	2.13±0.16	0.28±0.03	1.34±0.36	0.31±0.03
	100	0.75±0.06	0.11±0.02	0.86±0.06	2.06±0.16	0.07±0.01	2.13±0.16	0.36±0.04	1.55±0.42	0.40±0.04
P2-A1	0	0.60±0.07	0.24±0.05	0.84±0.08	1.23±0.10	0.34±0.04	1.57±0.11	0.49±0.07	0.71±0.18	0.54±0.07
	25	0.76±0.08	0.20±0.04	0.96±0.09	1.73±0.13	0.28±0.04	2.01±0.14	0.44±0.06	0.73±0.19	0.48±0.05
	50	0.83±0.09	0.07±0.02	0.90±0.09	2.39±0.20	0.12±0.02	2.51±0.20	0.35±0.05	0.58±0.19	0.36±0.05
	75	1.88±0.14	0.03±0.02	1.91±0.14	2.48±0.18	0.15±0.02	2.63±0.18	0.76±0.08	0.22±0.16	0.73±0.07
	100	0.56±0.08	0.03±0.02	0.59±0.08	2.49±0.18	0.12±0.02	2.61±0.18	0.23±0.03	0.22±0.13	0.22±0.03
P2-A3	0	1.16±0.08	0.53±0.05	1.68±0.09	1.53±0.11	0.32±0.04	1.85±0.12	0.75±0.08	1.67±0.26	0.91±0.08
	25	1.18±0.08	0.22±0.04	1.40±0.09	1.67±0.13	0.39±0.05	2.06±0.14	0.71±0.07	0.56±0.12	0.68±0.06
	50	1.00±0.09	0.06±0.02	1.05±0.09	2.75±0.21	0.19±0.03	2.94±0.21	0.36±0.04	0.30±0.10	0.36±0.04
	75	0.52±0.06	0.15±0.02	0.67±0.07	2.41±0.18	0.13±0.02	2.54±0.18	0.22±0.03	1.19±0.24	0.27±0.03
	100	2.25±0.13	0.10±0.01	2.35±0.13	3.29±0.26	0.07±0.01	3.36±0.26	0.68±0.07	1.43±0.35	0.70±0.07
P2-A5	0	0.55±0.06	0.17±0.02	0.72±0.07	2.57±0.20	0.28±0.04	2.85±0.21	0.21±0.03	0.60±0.12	0.25±0.03
	25	1.05±0.08	0.12±0.04	1.17±0.09	2.07±0.16	0.34±0.04	2.41±0.17	0.51±0.06	0.37±0.12	0.49±0.05
	50	0.93±0.08	0.15±0.02	1.08±0.08	2.70±0.21	0.28±0.04	2.98±0.21	0.34±0.04	0.55±0.11	0.36±0.04
	75	0.45±0.06	0.33±0.04	0.78±0.07	3.33±0.25	0.13±0.02	3.46±0.25	0.13±0.02	2.65±0.61	0.23±0.03
	100	0.75±0.08	0.10±0.02	0.85±0.08	4.00±0.30	0.07±0.01	4.07±0.30	0.19±0.02	1.42±0.42	0.21±0.03

Table S2 The export flux of POC from the euphotic zone based on $^{210}Po/^{210}Pb$ and $^{234}Th/^{238}U$ disequilibria

Region	latitude	Export interface/m	$^{210}Po/^{210}Pb)_{A.R.}$ *	^{234}Th–POC flux * / ($mmol \cdot m^{-2} \cdot d^{-1}$)	^{210}Po–POC flux * / ($mmol \cdot m^{-2} \cdot d^{-1}$)	References
Aleutian Basin	64 ºN–65ºN	100	0.05–1.32 (avg. 0.65)	nd	0.6–1.7 (avg. 1.1)	Hu et al. (2014)
Mediterranean Sea	40 ºN–45ºN	200	nd	3.8–17.5 (avg. 9.7)	4.4–7.0 (avg. 5.7)	Stewart et al. (2007a, 2007b)
Sargasso Sea	30 ºN–32ºN	150	0.21–0.94 (avg. 0.53)	0.3–24.5 (avg. 9.3)	2.4–9.1 (avg. 4.7)	Kim and Church (2001)
Antarctic Circumpolar Current	47ºS–57ºS	100	0.47–0.99 (avg. 0.66)	3.9–38.4 (avg. 16.7)	4.8–17.1 (avg. 10.8)	van der Loeff et al. (1997); Friedrich and van der Loeff (2002)
Bellingshausen Sea	67ºS	100	0.58–1.12 (avg. 0.82)	21	2.2	Shimmield et al. (1995)
Prydz Bay	64ºS	100	nd	nd	2.3	Yang et al. (2009)
Prydz Bay	64ºS–68ºS	100/200	0.36–1.20 (avg. 0.65)	nd	4.2–9.0 (avg. 6.9)	Hu et al. (2021)
Prydz Bay	62ºS–69ºS	100	0.21–1.16 (avg. 0.53)	nd	1.8–4.4 (avg. 2.9)	This study

Notes: * Value in parentheses indicate average value; nd represents no data